Estimating Soil Moisture, Inundation, and Methane Emissions from Siberian Wetlands using Models and Remote Sensing

Theodore J. Bohn[1], Erika Podest[2], Kyle C. McDonald[2], Chun-mei Chiu[3], Laura C. Bowling[3], and Dennis P. Lettenmaier[1]

[1]University of Washington, Seattle, Washington, USA; [3]JPL-NASA, Pasadena, California, USA; [3]Purdue University, West Lafayette, Indiana, USA

American Geophysical Union Fall Meeting, San Francisco, CA, USA, Dec 15-19 2008

Abstract

Estimation of methane emissions from high-latitude wetlands and changes that may occur in a warming climate is an important component of projections of global warming, due to the strength of methane as a greenhouse gas and the substantial fraction of global methane emissions that come from high latitudes. Efforts to monitor high-latitude methane emissions are hampered by the sparseness of in situ data at high latitudes, and in Northern Eurasia in particular. While biogeochemical modeling can provide estimates of methane emissions in areas where in situ measurements are scarce, the lack of in situ measurements also makes it difficult to calibrate and/or constrain these models. However, remote sensing products based on synthetic aperture radar that can be used to calibrate or constrain biogeochemical models in these regions at high resolution over multiple seasons have recently become available. We compare multi-temporal remotely-sensed estimates of saturated soil extent and inundation from the ALOS/PALSAR L-band sensor to simulations from our modeling framework (consisting of the Variable Infiltration Capacity macroscale hydrological model (VIC), extended to include carbon cycling and coupled to a methane emissions model) of these same quantities at multiple points in time over two growing seasons (2006 and 2007) for various locations in the West Siberian Lowlands. We assess the accuracy and precision of the model parameterization of water table distribution and examine the interannual variability of simulated inundation and methane emissions for the period 1948-2007.

1. Modeling Approach

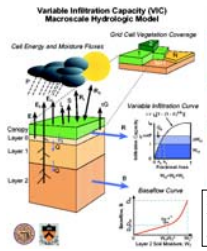

Figure 1: VIC overview and the VIC lake and wetland algorithm schematic.

Land Surface Hydrology Model
- Variable Infiltration Capacity (VIC) Model (Liang et al. 1994)
- Water and energy balance closure
- Macroscale: grid cells range from 10 to 100 km
- Statistical parameterizations of sub-grid variability in soil moisture, land cover
- Lake/wetland model (Bowling, 2002) handles changes in lake extent
- Grid cell average water table computed as sum of total column soil moisture deficit
- Extended to handle carbon cycling with photosynthesis, plant respiration, and NPP from BETHY (Knorr, 2000)

Sub-grid Variability of Water Table and Inundation
- Uses topographic wetness index formulation from TOPMODEL (Beven and Kirkby, 1979)
- Relates local water table position to local topography and the average water table depth of the region

Start with DEM (e.g. SRTM3)

For each pixel, define ***topographic wetness index*** $\kappa_i = \ln(\alpha_i/\tan\beta_i)$
α_i = upslope contributing area
$\tan\beta_i$ = local slope

Local water table depth
$Zwt_i = Zwt_{mean} - m(\kappa_i - \kappa_{mean})$
m = calibration parameter

Steep → **low** κ, **deep** Zwt

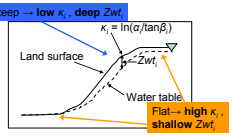

Flat→ **high** κ, **shallow** Zwt_i

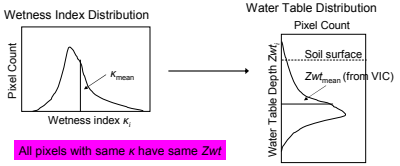

All pixels with same κ have same Zwt

Methane Model
- Walter and Heimann (2000) with modifications described in Walter et al (2001a)
- soil methane production, and transport of methane by diffusion, ebullition, and through plants modeled explicitly
- methane production occurs in the anoxic soil from the bottom of the soil column to the water table
- methane production rate controlled by soil temperature and NPP (both from VIC)
- methane oxidation also taken into account

Model Framework
- Gridded meteorological forcings drive the VIC hydrologic model
- VIC produces daily Zwt_{mean}, Soil T, and NPP
- Wetness index distribution from SRMT3 DEM, combined with Zwt_{mean}, gives distribution of Zwt
- Distributed Zwt(x,y), SoilT, and NPP drive methane model, which produces CH4(x,y)

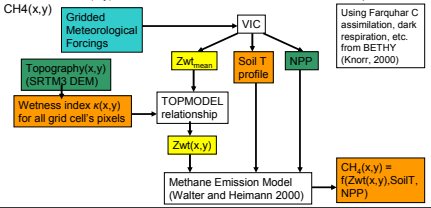

2. Study Domain

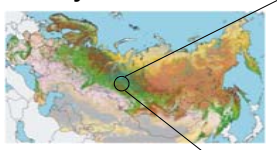

Our current study domain, shown in panel (a), is the Chaya/Bakchar/Iksha watershed in Siberia, which contains part of the vast Vasyugan Wetland complex. We will eventually extend our investigation to the entire West Siberian Lowlands, home to a large portion of the world's wetlands.

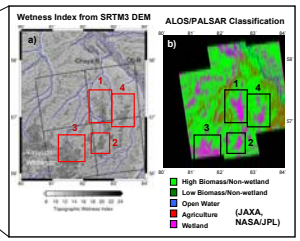

We are running our modeling framework at a resolution of 100km (EASE grid equal-area polar projection) (grid cells outlined in panel (a)). Topography is supplied by the SRTM 30m UTM DEM. For comparison with simulations, and to calibrating the modeling framework, we have classified 12.5m UTM PALSAR imagery from the region (panel (b)), acquired in the summers of 2006-07. Classes of particular interest are: open water and saturated/inundated land (with emergent vegetation) (listed as "wetland" in the legend in panel (b)). To calibrate the water table parameterization, we have selected 4 regions of interest (ROIs), shown as numbered boxes in panels (a) and (b).

3. Evaluating the Lateral Distribution of Inundation

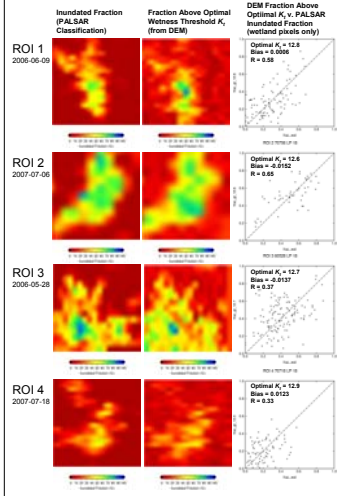

The TOPMODEL parameterization of the water table distribution must be calibrated. Here, we use remote sensing observations for calibration, in a two-step process:

1. Translate the observed inundated fraction to a threshold value of wetness index (κ_i), above which a pixel has water table above the soil surface

2. Estimate the value of the scaling factor m required to achieve a water table depth of 0 cm for a pixel having wetness index at the threshold value κ_i

Step 1 is described here; step 2 is described in section 4.

For each of the ROIs in fig. 2, we aggregated the remote sensing classifications up to 2700m resolution, computing the fraction of inundated 12.5m pixels in each 2700m "cell". Examples of observed inundation at each of the ROIs are shown in the first column of fig. 3, along with acquisition dates.

Before analyzing topography, we first smoothed the DEM with a cutoff wavelength of 2100 m, to reduce noise in the DEM caused by its coarse (1 m) vertical resolution and the effects of scattered tree canopies on the DEM. Then we computed wetness index values at all 30 m pixels of the smoothed DEM.

For each ROI, we aggregated to 2700 m resolution, computing the fraction of 30 m DEM pixels having wetness index κ_i > threshold κ_i within each 2700 m cell, for a range of threshold κ_i values. For each κ_i value, we evaluated the bias: mean(fraction >= κ_i) - mean(fraction_inundated). We then selected the κ_i value for which bias was smallest as the "best" estimate for that ROI and date. Maps of fraction above threshold at each of the ROIs on the same dates as the observations are shown in the second column of fig. 3.

Scatter plots of fraction >= κ_i vs. observed inundated fraction are shown in column 3 of fig. 3, for each ROI and date. Optimal κ_i values, bias, and correlation coefficient r are also listed for each ROI and date. Forest pixels have been masked out of these comparisons, since inundation under the forest canopy is difficult to observe and variation in forest canopy height introduces false topography into the DEM in these locations.

While the plots look visually similar, correlation coefficients are lower than expected, ranging from 0.33 to 0.65. The TOPMODEL formulation is a large-scale approximation and we do not expect complete correspondence. However, our spatial distributions appear to capture the general shape of wet areas at the landscape scale.

4. Calibrating the Vertical Distribution of Water Table

4.1 Local Calibration, Bakchar, 1999

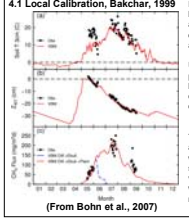

(From Bohn et al., 2007)

For this study, we use the same parameters for the VIC hydrologic model and methane emissions model of Walter and Heimann (2000) derived from calibration against in situ observations at a point in the Bakchar Bog in 1999 (Bohn et al., 2007; Friborg et al., 2003) (Fig. 4.1).

Using these parameters, we can estimate the TOPMODEL m parameter by comparing simulated water table position z_{wt} to best-fitting threshold wetness index values κ_i at the ROIs described in section 3. From the centroid of the scatter plot of z_{wt} vs. ($\kappa_i - \kappa_{mean}$) (Fig. 4.2), we estimate m as

m = mean(0 - z_{wt})/mean(κ_i - κ_{mean}) = 574 mm

There is clearly a large degree of scatter in fig. 4.2. This arises both from geographic differences among the ROIs as well as some lack of correlation between time series of simulated z_{wt} and "observed" κ_i. It is likely that both the κ_i values and the simulated z_{wt} contain error, and it would be worthwhile to investigate the effects of these errors on our results.

4.2 Simulated z_{wt} v. Best-Fit (κ_i - κ_{mean}) at All ROIs, 2006-2007

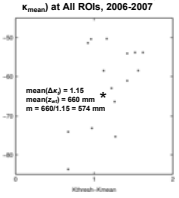

5. Interannual Variability

Fig. 5. Annual time series of relevant variables, Chaya basin, 1948-2007

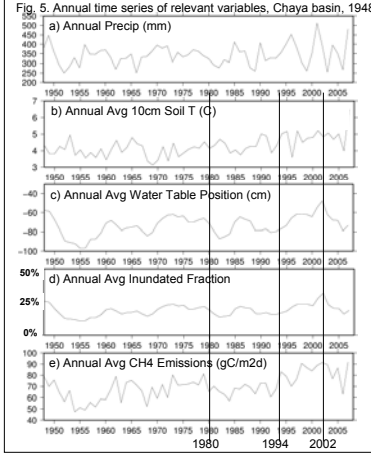

Using the parameters described in sections 3 and 4, we have run simulations for the Chaya/Bakchar/Iksha basin for the period 1948-2007. Meteorologic inputs were generated from gridded observations according to the procedure of Adam et al. (2007). The resulting time series of annual precipitation, average 10 cm soil temperature, average water table position, average inundated fraction, and average methane emissions are shown in fig. 5 a-e.

It can be seen that annual methane emissions (fig. 5.e.) respond to both soil temperature (fig. 5.b.) and basin-wide water table position (fig. 5.c.) (or inundated fraction (fig. 5.d.), which is non-linearly dependent on water table position).

We have not yet performed statistical analyses on the data. However, we can identify several areas that warrant examination:

1. There appears to be a positive trend in soil temperature since the late 1960s (fig 5.b.). This trend also appears to be present in the methane emissions. We would expect that trends in summer temperatures would directly affect methane emissions via changes in metabolic rates, and indirectly via changes in water table depth (through evaporation rates). Meanwhile, trends in winter temperatures would affect snow pack accumulation rates and the timing and strength of spring snow melt. A trend analysis of not only annual average values but also of seasonal values could help us understand which climate factors exert the most influence on methane emissions rates.

2. Basin-average water table position appears to exhibit some correlation with annual precipitation, along with some degree of interannual persistence, which can be expected in reservoirs with residence times longer than one year. It would be interesting to examine the autocorrelation of water table position and methane emissions, for a variety of possible model soil parameterizations, to assess their potential effects on interannual variability of methane emissions.

Three years, 1980, 1994, and 2002 have been identified in fig. 5. for discussion in section 6, below. 1980 represents an "average" year, with temperature and water table in the middle of their ranges. 2002 is a "warm, wet" year with extremely high water table and warmer than average temperature. 1994 is a "warm, dry" year, with high temperature but slightly lower than average water table.

6. Spatial Variability of Inundation and Methane Emissions

Fig. 6. Simulated Inundated Fraction and CH4 Emissions for Selected Years

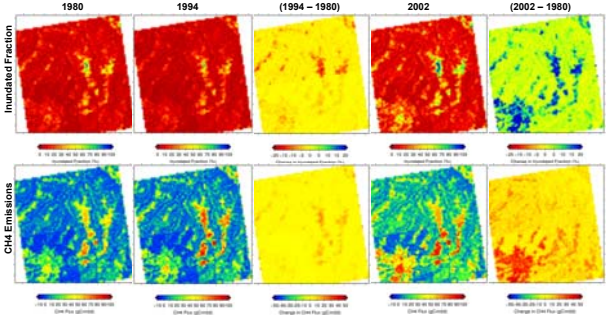

1994: A Warm, Dry Year

Inundation decreased, especially in the north of the basin, due to increased evaporation.

CH4 emissions increased via increased metabolic rates in response to higher temperatures, despite the reduction in inundated area. An exception to this is the lower left grid cell, which was so dry to begin with that the increase in metabolic rates did not help.

Responses of CH4 Emissions to T and P

1980: An "Average" Year

Inundation and CH4 emissions are strongest in bogs, as we would expect.

Lower-left 100km grid cell is drier than the others, and has accordingly lower CH4 emissions.

2002: A Warm, Wet Year

Inundation increases occurred consistently throughout the bogs, in all grid cells.

Increases in CH4 emissions also occurred throughout the bogs. However, lower-left grid cell emissions increased more than the others.

Take-away point: most variation of both inundation and CH4 emissions occurs in the wettest areas, i.e. bogs, in part because inundation is non-linear function of water table.

7. Conclusions and Future Work

Conclusions
- The TOPMODEL approximation gives a good fit to the spatial distribution of wetlands, offering a relatively inexpensive method for increasing the accuracy of methane emissions estimates from global large-scale models
- One benefit of the TOPMODEL parameterization is that it allows us to convert simulated water table depth into inundated extent, which can be observed by satellite
- Combining remote sensing data and models allows us to better understand the behavior of wetlands across vast, relatively inaccessible areas
- The ability to validate with remote sensing offers possibility of data assimilation schemes to enhance real-time monitoring

Future Work
- Explore the effects of errors in the TOPMODEL parameterization, and uncertainty in model parameter values, on simulated inundated extent and CH4 emissions
- Explore the statistical relationships among T, P, Zwt, inundation, and CH4 emissions over the period 1948-2007, including trend analysis and persistence
- Explore spatial variation in sensitivity of methane emissions to climate factors and parameter uncertainty, and identify areas where future observations might be most beneficial
- Extend analysis to all of West Siberian Lowlands

* References available upon request